

**Interfacial exchange coupling in Fe/(Ga,Mn)As bilayers**A. M. Alsmadi,<sup>1,2,3,\*</sup> Y. Choi,<sup>4</sup> D. J. Keavney,<sup>4</sup> K. F. Eid,<sup>3</sup> B. J. Kirby,<sup>5</sup> X. Liu,<sup>6</sup> J. Leiner,<sup>6,7</sup> K. Tivakornsasithorn,<sup>6,8</sup> M. Dobrowolska,<sup>6</sup> and J. K. Furdyna<sup>6</sup><sup>1</sup>*Department of Physics, Kuwait University, 13060 Safat, Kuwait*<sup>2</sup>*Department of Physics, The Hashemite University, 13115 Zarqa, Jordan*<sup>3</sup>*Department of Physics, Miami University, Oxford, Ohio 45056, USA*<sup>4</sup>*Advanced Photon Source, Argonne National Laboratory, Argonne, Illinois 60439, USA*<sup>5</sup>*Center for Neutron Research, National Institute for Standard Technology, Gaithersburg, Maryland 20899, USA*<sup>6</sup>*Department of Physics, University of Notre Dame, Notre Dame, Indiana 46556, USA*<sup>7</sup>*Quantum Condensed Matter Division, Oak Ridge National Laboratory, Oak Ridge, Tennessee 3783, USA*<sup>8</sup>*Department of Physics, Faculty of Science, Mahidol University, Bangkok 10400, Thailand*

(Received 26 February 2014; revised manuscript received 27 May 2014; published 16 June 2014)

We carried out a systematic study of magnetic order and magnetic interlayer coupling in Fe/(Ga,Mn)As bilayers using superconducting quantum interference device magnetometry, polarized neutron reflectometry, element-specific x-ray absorption spectroscopy, x-ray magnetic circular dichroism, and x-ray specular reflectivity. Our results clearly show that Fe/(Ga,Mn)As bilayers are strongly exchange coupled at the interface. However, contrary to recent reports in the literature, we observe a ferromagnetic rather than antiferromagnetic coupling between the magnetic moments of the Mn ions and the Fe layer. It is interesting in this context that the surface region of the (Ga,Mn)As layer that is in direct contact with the Fe film displays a nearly identical coercivity to that of Fe (indicating perfect ferromagnetic coupling of that region), while the bulk of the (Ga,Mn)As layer, which is more weakly ferromagnetically coupled with Fe, shows a significantly smaller coercive field.

DOI: [10.1103/PhysRevB.89.224409](https://doi.org/10.1103/PhysRevB.89.224409)

PACS number(s): 75.50.Pp, 75.25.-j, 78.70.Dm

**I. INTRODUCTION**

Studies of interfacial coupling between ferromagnetic (FM) films are important because of their fundamental physical interest, and, additionally, because such coupling can be used as a means of controlling the spin polarization of currents in spintronic devices [1]. These properties are now well understood in multilayers consisting of metallic FM constituents [2]. By comparison, magnetic coupling in heterostructures involving combinations of a FM metal layer and a FM semiconductor have been studied to a much lesser degree. Such combinations are, however, quite important because of their potential for electronic applications, particularly in systems where the ferromagnetic metal layer can be used as a spin injector or a spin filter coupled to a semiconductor device [3–6].

A representative example of such metal/semiconductor heterostructures is the hybrid combination of a Fe film deposited epitaxially on a FM semiconductor such as (Ga,Mn)As. This combination is unique in that it is made possible by the fortuitous lattice match between the (001) faces of the bcc Fe and the fcc semiconductor GaAs [7–9] [and therefore also (Ga,Mn)As], thus allowing fabrication of thin Fe/(Ga,Mn)As heterostructures of exceptional crystalline quality. Although hybrid systems such as Fe/GaMnAs, consisting of a canonical ferromagnet and an important FM semiconductor, have not been as thoroughly explored as their fully metallic or fully semiconductor counterparts [10–13], they have already attracted considerable interest both because of the basic properties of FM bilayers created in this way, and because of the potential for spintronic applications of this monolithic metal/semiconductor system [14,15].

In this paper we focus on exchange coupling between Fe and (Ga,Mn)As in Fe/GaMnAs bilayers grown by molecular beam epitaxy (MBE). To establish the physical properties of such hybrid bilayers, we carried out systematic experimental studies of this system using dc magnetization measurements, polarized neutron reflectometry, element-specific x-ray magnetic circular dichroism, x-ray absorption, and x-ray specular reflectivity measurements. We find that, contrary to recent reports in the literature [10], the Fe/(Ga,Mn)As bilayers used in this investigation display a ferromagnetic rather than antiferromagnetic exchange coupling between the two constituent FM materials. We explain this behavior in terms of the possible enriched concentration of Mn ions at the Fe/(Ga,Mn)As interface.

**II. SAMPLE FABRICATION**

The (Ga,Mn)As/Fe bilayers used in this study were grown by molecular beam epitaxy (MBE) on semi-insulating GaAs (001), as follows. After deoxidizing the substrate in the MBE chamber, a GaAs buffer of 100 nm thickness was first deposited on the substrate at a temperature of 590°C. The substrate was then cooled to 250°C, and a 2 nm GaAs buffer was grown at that low temperature, followed by deposition of (Ga,Mn)As with a nominal 6% Mn concentration to a thickness of ~100 nm. The substrate temperature was then reduced to 25°C, and a thin layer of Fe was deposited using an *e*-beam evaporator as the Fe source. The Fe film was finally capped with 2–3 nm of Au. Following this procedure, we grew three (Ga,Mn)As/Fe bilayer samples, with Fe layer thicknesses of 3, 4, and 8 nm.

During the growth, the surface of the layers was continually monitored by reflection high-energy electron diffraction (RHEED). Throughout the deposition of the entire multilayer structure we observed perfect crystalline growth, without any indication of cluster formation. Note that the nominal

\*Corresponding author: [abdel.alsmadi@ku.edu.kw](mailto:abdel.alsmadi@ku.edu.kw)

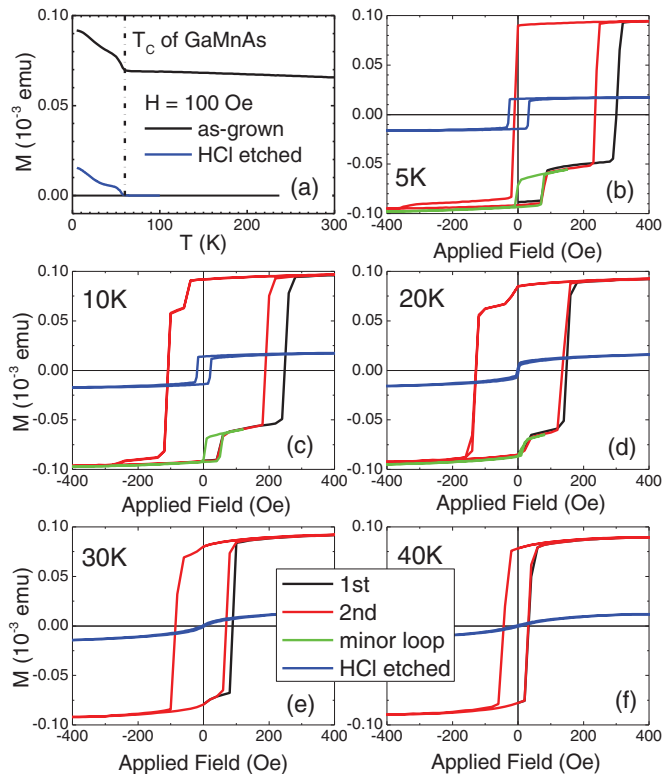


FIG. 1. (Color online) (a) Temperature dependence of magnetization data for a Fe(4 nm)/(Ga,Mn)As(100 nm) bilayer at  $H = 100$  Oe. (b)–(f) Full magnetization hysteresis loops measured by SQUID at various temperatures (black and red curves). The sample was zero-field cooled, with a negative magnetization of Fe along the [110] crystallographic direction due to a small residual field ( $\sim 2$  Oe) in the SQUID system. Minor hysteresis loops ascribed to the (Ga,Mn)As layer are shown in green. Blue curves in (b)–(d) show bulk (Ga,Mn)As magnetizations measured after etching away the Fe film.

thicknesses of Fe and Au are estimated from the ion current of the  $e$ -beam evaporator, which has a large uncertainty ( $\sim 30\%$ ) due to possible flux instabilities. The nominal thicknesses of the semiconductor layers were obtained from growth rates calibrated via RHEED oscillations, with an error estimated at less than 10%.

### III. EXPERIMENTAL MEASUREMENTS AND RESULTS

#### A. Static magnetometry

Static magnetic properties of the Fe/(Ga,Mn)As hybrid structures were determined using a superconducting quantum interference device (SQUID) magnetometer. The temperature dependence of the total magnetization of the Fe(4 nm)/(Ga,Mn)As(100 nm) bilayer is shown in Fig. 1(a), indicating that the Curie temperature of the (Ga,Mn)As layer of this sample is  $\sim 60$  K. Figure 1(a) also indicates that the magnetization of the Fe layer decreases slightly as the temperature increases up to 300 K.

Figures 1(b)–1(f) show the hysteresis loops  $M(H)$  of the bilayer measured at several temperatures. Prior to measuring the hysteresis, the sample was zero-field cooled (ZFC) to 5 K. The magnetic field in these measurements was applied in the

plane of the film, along the [110] direction. The field was initially swept from 0 to +400 Oe (training curve, shown in black), and then from +400 to  $-400$  Oe and back (red line). One should note that there is a finite net magnetization in the Fe film even after ZFC due to a weak residual field in the SQUID system (of the order of 2 Oe), causing a net *negative* magnetization at the starting point of the first field sweep, which results in a distinct two-step switching process, the first step occurring when the magnetization is reversed in the layer with a weaker coercive field. The two steps in magnetization reversal thus indicate different behavior of the Fe and the (Ga,Mn)As layers. Based on the temperature dependence of the magnetization loops, we attribute the first step in the magnetization sweep (smaller coercive field) to the (Ga,Mn)As layer, while the turning point of the hysteresis loop occurring at higher fields is ascribed to magnetization reversal in the Fe layer.

The total change in the magnetization at the two magnetization turning points has a ratio of  $\sim 15:4$ , which is reasonably consistent with both the magnetic moments and the thicknesses of the two FM layers. At lower temperatures ( $\leq 20$  K), the center of the hysteresis loop is shifted to the right of the zero-field axis, indicating the presence of exchange bias in the Fe film. We attribute the observed exchange bias to an antiferromagnetic Fe oxide at the Fe/Au interface formed by penetration of oxygen through the Au capping layer. Evidence for the formation of Fe oxide and its effects has already been extensively discussed elsewhere [16]. The presence of the exchange bias, and the enhancement of coercive field in the Fe film associated with this effect, shed additional light on the magnetic coupling between the Fe and the (Ga,Mn)As layers, discussed below.

In order to understand the behavior of the Fe/(Ga,Mn)As coupling in the bilayer, we measured the minor hysteresis loops of the (Ga,Mn)As film at 5, 10, and 20 K. The minor loops are shown in green in Figs. 1(b)–1(d) for positive fields, in the region where the magnetization of the Fe film during the forward sweep is pinned in the negative direction, thus shifting the minor (Ga,Mn)As loops downward. From the behavior of the minor loops we infer that the magnetic coupling between Fe and (Ga,Mn)As film is characterized as a weak *ferromagnetic* type. This is evident, for example, in the sweep in the positive field direction, where the negative magnetization of the (Ga,Mn)As layer is aligned with the negative magnetization of the Fe film at zero field, but a weak positive field of the order of several tens of Oe is sufficient to reverse it.

In order to verify that the minor loop seen in green in Figs. 1(b)–1(d) indeed corresponds to the contribution of the bulk (Ga,Mn)As component, we etched away the Fe layer from the bilayers, which allowed us to measure the magnetization of the (Ga,Mn)As layer alone, thus revealing its bulk properties without the effect of the adjacent Fe layer. The results are shown in Fig. 1 in blue color. It is clear that the minor loop seen in the Fe/(Ga,Mn)As bilayer is now centered at zero field. The fact that the amplitude and the hysteresis width of that loop matches closely that of the minor loop of the bilayer provides further corroboration that the minor loop of the bilayer represents the contribution of bulk (Ga,Mn)As at all temperatures. This confirms the conjecture made in the paper

that the minor loop indeed represents the magnetization of the bulk (Ga,Mn)As layer, superimposed on the exchange-biased hysteresis of the Fe layer, and coupled ferromagnetically to that layer at equilibrium.

### B. Polarized neutron reflectometry

Polarized neutron reflectometry (PNR) measurements were performed using the NG-1 Reflectometer at the NIST Center for Neutron Research. The measurements were conducted on a similar sample [Fe(3 nm)/(Ga,Mn)As(27 nm)] to confirm the nature of the coupling between the Fe and (Ga,Mn)As layers. Specular PNR is directly sensitive to the nuclear and the in-plane magnetization depth profiles of thin films and multilayers, thus allowing us to directly distinguish the (Ga,Mn)As magnetization from that of Fe. At room temperature [i.e., well above the (Ga,Mn)As Curie temperature] the Fe was magnetized along the “+” direction,  $18^\circ$  away from the [110] direction of GaAs substrate, and the sample was cooled to 5 K in a  $-10$  Oe magnetic field (opposite to the Fe magnetization direction). Without changing the field, PNR spectra were then measured as a function of increasing temperature. The incident neutron beam was polarized to be spin up or spin down with respect to the applied field direction, and both non-spin-flip (NSF) and spin-flip (SF) reflectivities were measured as a function of wave vector transfer  $Q$ .

The sample magnetization manifested itself in neutron scattering both as a splitting of the NSF cross sections (which arises from the component of the in-plane magnetization parallel to the applied field), and as nonzero SF cross sections (indicative of the component of the in-plane magnetization perpendicular to the applied field) [17]. Typical NSF data measured at 5 and 60 K are shown in Fig. 2(a), plotted as spin asymmetry (i.e., the difference between spin-up and spin-down signals divided by their sum), while the corresponding SF data (the average of the up-down and down-up cross sections) are shown in Fig. 2(b). Using the REFLID software package [18], the data are well fit by a simple model featuring a GaAs substrate, 27 nm of (Ga,Mn)As, 3 nm of Fe, and 3 nm of Au, with *both* the Fe and (Ga,Mn)As magnetizations parallel to each other.

The temperature-dependent magnetizations of each layer as determined from the model fitting are shown in Fig. 2(c). The Fe magnetization is essentially constant from 5 to 60 K, while the (Ga,Mn)As magnetization decreases with increasing temperature. These results indicate that, as the sample is cooled in the  $-10$  Oe field, the Fe magnetization rotates toward an in-plane easy axis direction, and below its Curie temperature the (Ga,Mn)As is magnetized along the same direction. That the (Ga,Mn)As layers spontaneously magnetize parallel to Fe even in the presence of a small opposing field strongly suggests the presence of ferromagnetic coupling between the Fe and the (Ga,Mn)As layers.

### C. Element-specific x-ray absorption and x-ray magnetic circular dichroism

X-ray absorption spectroscopy (XAS) and x-ray magnetic circular dichroism (XMCD) experiments were carried out at the 4-ID-C beamline of the Advanced Photon Source (APS)

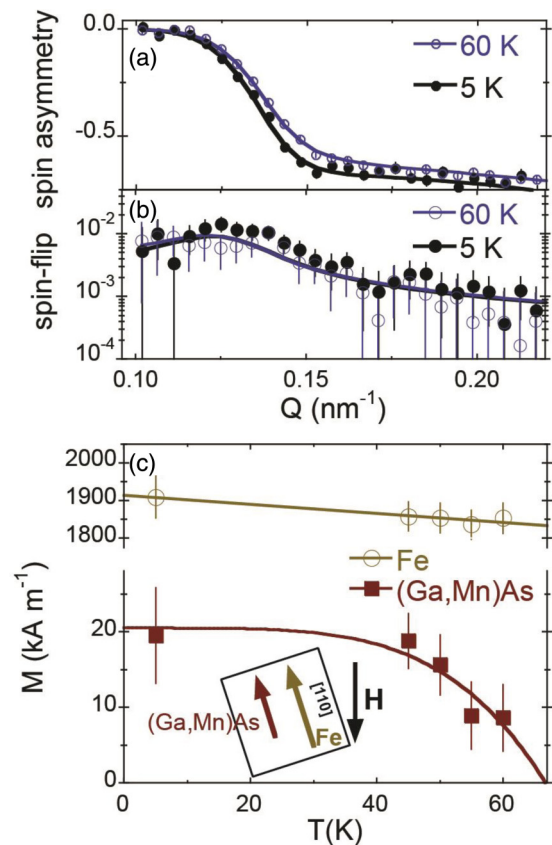


FIG. 2. (Color online) Examples of (a) neutron NSF data and fits (plotted as spin asymmetry), and (b) neutron SF data and fits. (c) Temperature dependence of magnetization data for the Fe and (Ga,Mn)As layers, as determined from the fits. Lines in (c) are linear and power-law fits are intended as guides to the eye.

at Argonne National Laboratory. XAS/XMCD measurements in total electron yield (TEY), fluorescence yield (FY), and reflectivity (REF) were acquired simultaneously at a  $4^\circ$  grazing incident angle with respect to the sample surface. The XAS and XMCD measurements were performed at the  $L_{2,3}$  edges of Fe, Mn, and Ga on Fe/(Ga,Mn)As samples with two Fe thicknesses (4 and 8 nm). The measurements were performed at room temperature and at 4 K after zero-field cooling.

Typical results of XAS and XMCD are shown in Fig. 3. The data taken in the TEY mode are shown in red, and the FY measurements, which are more bulk sensitive than the TEY mode, are shown in black [19,20]. All spectra are normalized by the intensity of the incident beam. Figure 3(a) shows normalized Fe  $L_{2,3}$  XAS  $(I^+ + I^-)/2$  spectra recorded at 4 K for Fe(4 nm)/Ga,Mn)As(100 nm), where  $I^+$  and  $I^-$  indicate intensities of two counter-rotating circular polarizations of the x-ray beam. In TEY and FY modes, XAS measurements show a clear splitting in the Fe  $L_3$  absorption peak, which is a direct signature for the formation of an Fe oxide at the Au/Fe interface, as was reported earlier [16], a result that is also directly relevant to our interpretation of the exchange bias observed at low temperatures, seen in Fig. 1.

Since the splitting of the Fe  $L_{2,3}$  peak signals the presence of an Fe oxide, it is important to ask whether oxidation [either of the Fe layer, or of Mn at the Fe/(Ga,Mn)As interface] could

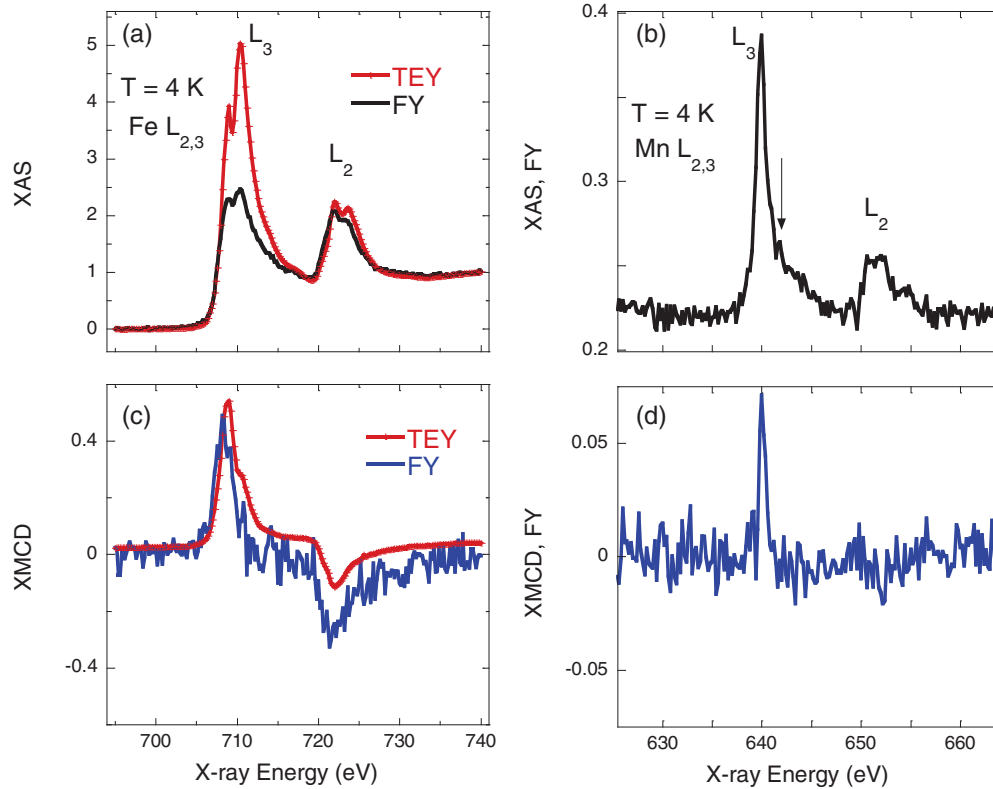


FIG. 3. (Color online) Fe and Mn normalized XAS ( $I^+ + I^-$ )/2 and XMCD ( $I^+ - I^-$ ) spectra recorded at 4 K after zero-field cooling for Fe/(Ga,Mn)As bilayers with 4 nm Fe, 100 nm (Ga,Mn)As. Spectra in (a) and (c) are measured at the Fe  $L_{2,3}$  edge using TEY (red line) and FY (black line) detection modes. (b) and (d) are FY data measured at the Mn  $L_{2,3}$  edge. XAS and XMCD were measured with an applied field of 800 Oe. TEY data for the Mn edge are not included, because absorption of electrons by the Fe and Au layers makes that signal too weak to be meaningfully distinguished from the noise.

affect the FM coupling between the Fe and the (Ga,Mn)As layers discussed in this paper. We can, however, rule out this effect as follows. First, the oxidation takes place after the sample is taken out of the growth chamber, and is therefore expected to occur on the outer surface of the relatively thick (4 nm) Fe layer. The fact that the same magnetic behavior, indicative of FM coupling between Fe and (Ga,Mn)As, is also observed in an Fe/(Ga,Mn)As bilayer with an 8 nm Fe film (see the Supplemental Material [21]) further supports this conclusion. Finally, effects of diffusion of oxygen through the Fe layer to its interface with (Ga,Mn)As can be additionally ruled out by the absence of Mn oxide signatures in the XAS signal observed at the Mn  $L_{2,3}$  edge in Fig. 3(b), as discussed below. From this we conclude that the coupling between Fe and (Ga,Mn)As occurring at their interface is representative of the two materials in their unperturbed form.

Figure 3(b) shows normalized Mn  $L_{2,3}$  XAS spectra recorded at 4 K for the same sample. In Mn  $L_{2,3}$  XAS, the  $2p$  core electrons are excited into the unoccupied  $3d$  states, providing a direct measurement of the electronic structure of the polarized Mn  $3d$  band. As shown in Fig. 3(b), the Mn  $L_{2,3}$  absorption spectra show a sharp line shape, similar to the spectra recently reported by others [10–12,22]; for the hybrid  $d^4-d^5-d^6$  configuration of Mn in the GaAs matrix. In addition, a small shoulder is observed at the high-photon energy side of the main peak (indicated by an arrow). This shoulder may be due to interstitial Mn which is typically found

in (Ga,Mn)As, since interstitial Mn is expected to be more weakly screened than substitutional Mn, and should thus have its XAS peak at a higher photon energy [22]. This feature may prove to be important in future studies of Fe/(Ga,Mn)As since, as discussed below, accumulation of Mn interstitials in the interface region between Fe and GaMnAs may play a key role in the magnetic coupling of the two FM materials. Moreover, the Mn XAS spectra in our sample [Fig. 3(b)] do not show the distinct multiple structure characteristics for a highly localized  $d^5$  ground state that have been previously reported [10,23,24], which are typical for Mn oxides [10,22,25]. This is as expected, because the (Ga,Mn)As surface is covered by Fe in UHV, thus preventing Mn oxide formation. We note also that the Mn XAS data observed in our samples show a distinctly different behavior from XAS observed on Fe/Mn and other metallic Mn alloys [10,26]. We may therefore exclude any significant Mn segregation or Mn diffusion into the Fe layer, or the formation of a strongly intermixed Mn/Fe region [10,26].

Figures 3(c) and 3(d) show XMCD ( $I^+ - I^-$ ) spectra observed at 4 K for Fe(4 nm)/(Ga,Mn)As for Fe and Mn  $L_{2,3}$  edges, respectively. A magnetic field of 800 Oe was applied along the [110] direction of the bilayer during the measurement. The Fe film displays a strong XMCD signal at the  $L_{2,3}$  edges, while XMCD due to Mn is considerably weaker. We note parenthetically that XMCD at the Ga edge (data not shown) is negligibly small. The Fe XMCD asymmetry ratio [defined as  $(I^+ - I^-)/(I^+ + I^-)$ ] at the  $L_3$  edge

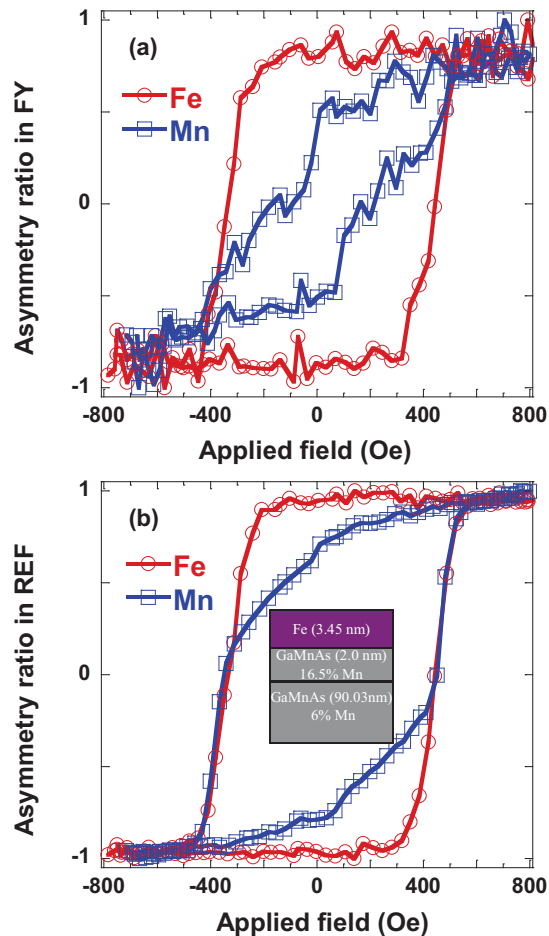


FIG. 4. (Color online) Element-specific asymmetry ratios  $(I^+ - I^-)/(I^+ + I^-)$  for the Fe(4 nm)/(Ga,Mn)As(100 nm) bilayer obtained at the  $L_{2,3}$  edges of Fe (red curves) and Mn (blue curves), revealing the hysteresis for the Fe and Mn magnetizations. Data were measured at 4 K after zero-field cooling, with an in-plane field along the [110] crystallographic direction. Measurements in the FY (a) and the REF modes (b) were taken simultaneously.

reaches a maximum of 30%, which is in good agreement with reported values at room temperature [10–12]. The Mn XMCD asymmetry value is about 15% at 4 K, considerably larger than results reported earlier [13,23], indicating that a larger number of the Mn ions is contributing to the magnetic order in our samples than expected from the nominal concentration of Mn in the (Ga,Mn)As layer, with excellent agreement with published results [21,26–31].

Element-specific magnetic hysteresis loops for Fe and Mn were obtained by recording the XMCD signal as a function of applied field at a fixed incident x-ray energy at the two absorption edges. In Fig. 4 we plot these hysteresis loops for a magnetic field along the [110] direction recorded at the  $L_3$  edges of Fe and Mn at 4 K. Similar behavior was observed in the remaining Fe/(Ga,Mn)As samples with different Fe thicknesses (see the Supplemental Material [21]). Figure 4(a) shows the asymmetry ratio  $(I^+ - I^-)/(I^+ + I^-)$  for data taken in the TEY mode, and Fig. 4(b) corresponds to data observed in the resonance REF mode, which is expected to be significantly more sensitive to the region directly at

the interface (see the Supplemental Material [21]). In both cases the hysteresis loop for the Fe edge displays a square hysteresis, with coercive fields of about 400 Oe, while the Mn loop is rather distorted, showing signatures of a two-step switching of magnetization [the two-step feature is clearer in Fig. 4(b), but close inspection of Fig. 4(a) also shows indications of such a two-step process]. For completeness, data obtained for sample Fe(8 nm)/(Ga,Mn)As are presented in the Supplemental Material [21]. It is significant for later discussions that the Mn hysteresis and the coercive fields observed in the REF mode [which is primarily sensitive to the near-surface region of (Ga,Mn)As] are nearly coincident with those of the Fe loop, while the Mn coercivity seen in the FY mode, which is more representative of bulk (Ga,Mn)As, is significantly narrower.

#### IV. DISCUSSION AND CONCLUDING REMARKS

The results of magnetization and PNR measurements presented above indicate the presence of ferromagnetic coupling between Fe and (Ga,Mn)As in the Fe/(Ga,Mn)As bilayers studied. Additionally, information on element-specific contributions to the magnetization profile at and near the Fe/(Ga,Mn)As interface was obtained from x-ray measurements which combine the depth-sensitive resolving power of conventional small-angle x-ray reflectivity with the element sensitivity of x-ray circular magnetic dichroism (XMCD) measured at the x-ray absorption edges of specific elements. The latter can be readily seen by comparing the XMCD results obtained in the REF and FY modes at the  $L_{2,3}$  absorption edges of Mn and Fe, shown in Fig. 4. Since in our specular reflection setup the REF mode is especially sensitive to the region immediately near the surface (see the Supplemental Material [21]), the differences between the Mn hysteresis loops observed by the REF and the FY modes (as seen in Fig. 4) indicate that the magnetization depth profile of Mn is not uniform near the Fe/(Ga,Mn)As interface. This can be explained by assuming that the (Ga,Mn)As layer consists of two regions: a thin Mn-rich (Ga,Mn)As surface region in direct contact with the Fe film, and a magnetically “softer” region corresponding to the bulk of the (Ga,Mn)As layer. The thin Mn-rich region exhibits a strong ferromagnetic coupling with the Fe layer (with nearly identical coercivity), as seen in Fig. 4(b). The bulk (Ga,Mn)As is also ferromagnetically coupled to Fe, but much more weakly, showing much weaker coercive fields [as seen in the FY data shown in Fig. 4(a), and in the narrow minor loops in Fig. 1].

It is instructive at this point to compare the general characteristics of the hysteresis loops measured by XMCD with the hysteresis data obtained from SQUID measurements. The hysteresis loops are wide in both cases, but XMCD are clearly symmetric about zero field, while low-temperature SQUID hysteresis loops are shifted by the exchange bias. The reason for this difference is that the SQUID data are obtained on very small specimens (less than  $3 \times 3$  mm), which essentially correspond to a single domain, while specimens used in XMCD are quite large, allowing for the existence of many domains at zero field. As was shown in Ref. [16], in zero-field-cooled uniaxially anisotropic thin Fe layers exchange bias can pin two independent FM domain populations

characterized by opposite exchange bias fields, as shown in Fig. 6 of Ref. [16]. Thus, in the presence of a large number of domains, one expects broad symmetric hysteresis loops resulting from the superposition of contributions from the two domain populations. In fact, careful examination of Figs. 1(b) and 1(c) indicates a trace amount of such opposite exchange bias also in the SQUID data taken at low temperatures. A random distribution of such oppositely biased domains would thus result in broad symmetric hysteresis loops, as is indeed observed in Fig. 4.

Both the SQUID data [where the (Ga,Mn)As contribution in the minor loop is dominated by the “bulk” interior of the (Ga,Mn)As layer] and the XMCD data observed at the Mn  $L_{2,3}$  absorption edge [which reflect the behaviors of the near-interface Mn-rich region of the sample and of the (Ga,Mn)As interior] indicate that the entire (Ga,Mn)As is ferromagnetically coupled to the Fe overlayer. This observation differs from several previous studies of Fe/(Ga,Mn)As bilayers [10–12], where an antiparallel alignment was observed between the Fe layer and the Mn moments in the bulk of the GaMnAs layer. However, a recent study of exchange coupling in such bilayers also revealed that the type of coupling [antiferromagnetic (AFM) or FM] depends strongly on the thickness of the (Ga,Mn)As layer [13], AFM coupling of bulk (Ga,Mn)As occurring in thick (Ga,Mn)As layers, and FM alignment becoming dominant when the (Ga,Mn)As layers become ultrathin (below about 10 nm in Ref. [13]).

A comparison of the data reported earlier and our present results appears to point to the importance of the Mn-rich layer at the Fe/(Ga,Mn)As interface for mediating the coupling between Fe and (Ga,Mn)As. We therefore discuss the origin and the expected properties of such interfacial layers. It is well known that Mn interstitials which form during the MBE growth of (Ga,Mn)As tend to diffuse to the (Ga,Mn)As surface [27]. This process occurs even during the MBE growth [27,28], and is thus responsible for an increased Mn concentration at the interface of Fe/(Ga,Mn)As in bilayers. In Ref. [27] it was also shown that in (Ga,Mn)As films with thicknesses below 60 nm, essentially all interstitials formed during the growth diffuse to the surface, while for thicker films a significant concentration of Mn<sub>i</sub> remains distributed within the bulk. Thus the supply of interstitials is depleted by outdiffusion in the bulk of (Ga,Mn)As layers for thicknesses below 60 nm, indicating that such layers will be less Mn rich in thinner samples, but the existence of Mn<sub>i</sub> within the bulk for thicknesses above that value suggests that the amount of Mn accumulated at the surface eventually levels off, and prevents further outdiffusion of Mn<sub>i</sub> to the near-surface region.

Based on this reasoning, we infer from Ref. [27] that the concentration of Mn at the interface of Fe and a (Ga,Mn)As film of ~100 nm is expected to be significantly higher than in the ultrathin (Ga,Mn)As layers comprising Fe/(Ga,Mn)As

bilayers used in earlier studies [13]. In an attempt to quantify the thickness of this interfacial Mn-rich region, we also carried out x-ray resonant reflectivity to gain information on the chemical depth profile of our multilayer structure (see the Supplemental Material [21]). The best fit of the reflectivity curves is obtained by assuming a ~2 nm (Ga,Mn)As layer with a concentration of Mn of 16.5% at the interface, and a thickness of ~90.0 nm for the remaining (Ga,Mn)As layer, with a Mn concentration of 6%. As noted above, it is possible that the ferromagnetic coupling which we observe is directly related to the high Mn concentration at the Fe/(Ga,Mn)As interface of our system, and that the AFM coupling occurring in Fe/GaMnAs bilayers involving much thinner (Ga,Mn)As films is a result of fewer Mn ions in this critical region.

It is important to point out that the interfacial Mn-rich layer acts very differently from the bulk (Ga,Mn)As, due to the influence of the immediately adjacent Fe. Specifically, in the grazing-incidence REF mode we observe finite XMCD at the Mn  $L_{2,3}$  edge up to room temperature with the same sign as the XMCD observed at the Fe absorption edge (see the Supplemental Material [21]), indicating that the magnetic behavior of the Mn accumulated at the interface is essentially locked to the ferromagnetic properties of the Fe layer. This is compatible with the results reported by earlier studies of the (Ga,Mn)As/Fe bilayers [10].

As noted, the observation that in the case of our (Ga,Mn)As/Fe bilayers comprising relatively thick (Ga,Mn)As films, the (Ga,Mn)As layer is ferromagnetically coupled to Fe, differs from results reported for this structure consisting of ultrathin (Ga,Mn)As. This points to the complexity of such hybrid systems, and particularly to the physics governing the Mn-rich interfacial layer formed by the outdiffusion of Mn interstitials to the surface of the (Ga,Mn)As. While the properties of such interfacial layers can in part be traced to the layer thickness [13], they are also expected to depend on the Mn content, termination of the (Ga,Mn)As layer adjacent to Fe, other details of the growth process, and possibly interdiffusion between the elements at the Fe/(Ga,Mn)As interface. Further work is clearly needed, aimed both at identifying the physical properties of such interfacial layers, and at an understanding of the role of such layers in mediating the nature of magnetic coupling between two ferromagnetic [in our case, Fe and (Ga,Mn)As] materials.

#### ACKNOWLEDGMENTS

The work at Notre Dame was supported by the National Science Foundation Grant No. DMR10-05851. The work at the Advanced Photon Source, an Office of Science User Facility operated for the U.S. Department of Energy (DOE) Office of Science by Argonne National Laboratory, was supported by the U.S. DOE under Contract No. DE-AC02-06CH11357.

[1] G. W. Fernando, in *Metallic Multilayers and Their Applications Theory, Experiments, and Applications Related to Thin Metallic Multilayers*, edited by G. W. Fernando, Handbook of Metal Physics Vol. 4 (Elsevier, Amsterdam, 2008).

[2] *Magnetic Heterostructures*, edited by H. Zabel and S. D. Bader (Springer, Berlin, 2008).

[3] G. A. Prinz, *Science* **250**, 1092 (1990).

[4] H. Ohno, *Science* **281**, 951 (1998).

- [5] S. A. Wolf, D. D. Awschalom, R. A. Buhrman, J. M. Daughton, S. von Molnár, M. L. Roukes, A. Y. Chtchelkanova, and D. M. Treger, *Science* **294**, 1488 (2001).
- [6] T. Dietl, *Nat. Mater.* **9**, 965 (2010).
- [7] J. J. Krebs, B. T. Jonker, and G. A. Prinz, *J. Appl. Phys.* **61**, 2596 (1987).
- [8] G. Wastlbauer and J. A. C. Bland, *Adv. Phys.* **54**, 137 (2005).
- [9] J. K. Furdyna and J. Kossut, *Superlattices Microstruct.* **2**, 89 (1986).
- [10] F. Maccherozzi, M. Sperl, G. Panaccione, J. Minár, S. Polesya, H. Ebert, U. Wurstbauer, M. Hochstrasser, G. Rossi, G. Woltersdorf, W. Wegscheider, and C. H. Back, *Phys. Rev. Lett.* **101**, 267201 (2008).
- [11] M. Sperl, F. Maccherozzi, F. Borgatti, A. Verna, G. Rossi, M. Soda, D. Schuh, G. Bayreuther, W. Wegscheider, J. C. Cezar, F. Yakhou, N. B. Brookes, C. H. Back, and G. Panaccione, *Phys. Rev. B* **81**, 035211 (2010).
- [12] K. Olejnik, P. Wadley, J. A. Haigh, K. W. Edmonds, R. P. Campion, A. W. Rushforth, B. L. Gallagher, C. T. Foxon, T. Jungwirth, J. Wunderlich, S. S. Dhesi, S. A. Cavill, G. van der Laan, and E. Arenholz, *Phys. Rev. B* **81**, 104402 (2010).
- [13] M. Sperl, P. Torelli, F. Eigenmann, M. Soda, S. Polesya, M. Utz, D. Bougeard, H. Ebert, G. Panaccione, and C. H. Back, *Phys. Rev. B* **85**, 184428 (2012).
- [14] H. J. Zhu, M. Ramsteiner, H. Kostial, M. Wassermeier, H.-P. Schönherr, and K. H. Ploog, *Phys. Rev. Lett.* **87**, 016601 (2001).
- [15] B. D. Schultz, N. Marom, D. Naveh, X. Lou, C. Adelman, J. Strand, P. A. Crowell, L. Kronik, and C. J. Palmström, *Phys. Rev. B* **80**, 201309(R) (2009).
- [16] K. Tivakornsasithorn, A. M. Alsmadi, X. Liu, J. C. Leiner, Y. Choi, D. J. Keavney, K. F. Eid, M. Dobrowolska, and J. K. Furdyna, *J. Appl. Phys.* **113**, 133908 (2013).
- [17] J. F. Ankner and G. P. Felcher, *J. Magn. Magn. Mater.* **200**, 741 (1999).
- [18] B. J. Kirby, P. A. Kienzle, B. B. Maranville, N. F. Berk, J. Krycka, F. Heinrich, and C. F. Majkrzak, *Curr. Opin. Colloid Interface. Sci.* **17**, 44 (2012).
- [19] R. Nakajima, J. Stöhr, and Y. U. Idzerda, *Phys. Rev. B* **59**, 6421 (1999).
- [20] A. A. Freeman, K. W. Edmonds, N. R. S. Farley, S. V. Novikov, R. P. Campion, C. T. Foxon, B. L. Gallagher, E. Sarigiannidou, and G. van der Laan, *Phys. Rev. B* **76**, 081201(R) (2007).
- [21] See Supplemental Material at <http://link.aps.org/supplemental/10.1103/PhysRevB.89.224409> for probing depth estimate for x-ray, in addition to extra XMCD and x-ray reflectivity measurements on Fe/GaMnAs bilayers.
- [22] K. W. Edmonds, N. R. S. Farley, R. P. Campion, C. T. Foxon, B. L. Gallagher, T. K. Johal, G. van der Laan, M. MacKenzie, J. N. Chapman, and E. Arenholz, *Appl. Phys. Lett.* **84**, 4065 (2004).
- [23] H. Ohldag, V. Solinus, F. U. Hillebrecht, J. B. Goedkoop, M. Finazzi, F. Matsukura, and H. Ohno, *Appl. Phys. Lett.* **76**, 2928 (2000).
- [24] S. Ueda, S. Imada, T. Muro, Y. Saitoh, S. Suga, F. Matsukura, and H. Ohno, *Physica E (Amsterdam)* **10**, 210 (2001).
- [25] Y. Ishiwata, M. Watanabe, R. Eguchi, T. Takeuchi, Y. Harada, A. Chainani, S. Shin, T. Hayashi, Y. Hashimoto, S. Katsumoto, and Y. Iye, *Phys. Rev. B* **65**, 233201 (2002).
- [26] K. W. Edmonds, A. A. Freeman, N. R. S. Farley, K. Y. Wang, R. P. Campion, B. L. Gallagher, C. T. Foxon, G. van der Laan, and E. Arenholz, *J. Appl. Phys.* **102**, 023902 (2007).
- [27] K. M. Yu, W. Walukiewicz, T. Wojtowicz, J. Denlinger, M. A. Scarpulla, X. Liu, and J. K. Furdyna, *Appl. Phys. Lett.* **86**, 042102 (2005).
- [28] K. W. Edmonds, P. Bogusławski, K. Y. Wang, R. P. Campion, S. N. Novikov, N. R. S. Farley, B. L. Gallagher, C. T. Foxon, M. Sawicki, T. Dietl, M. Buongiorno Nardelli, and J. Bernholc, *Phys. Rev. Lett.* **92**, 037201 (2004).
- [29] K. F. Eid, B. L. Sheu, O. Maksimov, M. B. Stone, P. Schiffer, and N. Samarth, *Appl. Phys. Lett.* **86**, 152505 (2005).
- [30] V. Holy, Z. Matej, O. Pacherova, V. Novak, M. Cukr, K. Olejnik, and T. Jungwirth, *Phys. Rev. B* **74**, 245205 (2006).
- [31] F. Maccherozzi, G. Panaccione, G. Rossi, M. Hochstrasser, M. Sperl, M. Reinwald, G. Woltersdorf, W. Wegscheider, and C. H. Back, *Surf. Sci.* **601**, 4283 (2007).